DMD Fast Forward. Published on September 11, 2019 as DOI: 10.1124/dmd.119.087262
This article has not been copyedited and formatted. The final version may differ from this version.

Title

Elucidation of N^1-methyladenosine as a potential surrogate biomarker for drug interaction studies involving renal organic cation transporters

Authors

Takeshi Miyake[1], Tadahaya Mizuno[1], Issey Takehara[2], Tatsuki Mochizuki[1], Miyuki Kimura[3], Shunji Matsuki[3], Shin Irie[3], Nobuaki Watanabe[4], Yukio Kato[5], Ichiro Ieiri[6], Kazuya Maeda[1], Osamu Ando[4], and Hiroyuki Kusuhara[1*]

Affiliations

[1]Laboratory of Molecular Pharmacokinetics, Graduate School of Pharmaceutical Sciences, the University of Tokyo, Tokyo, Japan

[2]Biomarker Department, Daiichi-Sankyo Co., Ltd., Tokyo, Japan

[3]Fukuoka Mirai Hospital Clinical Research Center, Fukuoka, Japan

[4]Drug Metabolism & Pharmacokinetics Research Laboratories, Daiichi-Sankyo Co., Ltd., Tokyo, Japan

[5]Faculty of Pharmacy, Institute of Medical, Pharmaceutical and Health Sciences, Kanazawa University

[6]Department of Clinical Pharmacokinetics, Graduate School of Pharmaceutical Sciences, Kyushu University, Fukuoka, Japan

DMD Fast Forward. Published on September 11, 2019 as DOI: 10.1124/dmd.119.087262
This article has not been copyedited and formatted. The final version may differ from this version.

Running Title

Endogenous probe of organic cation transporters

Corresponding Author

Hiroyuki Kusuhara, Ph.D.

Affiliation: Laboratory of Molecular Pharmacokinetics, Graduate School of Pharmaceutical Sciences, The University of Tokyo

Address: 7-3-1, Hongo, Bunkyo-ku, Tokyo 113-0033, Japan

Tel: +81-3-5841-4770; Fax: +81-3-5841-4766; Email: kusuhara@mol.f.u-tokyo.ac.jp

Numbers for manuscript elements

Text pages: 37

Number of tables: 6

Number of figures: 7

Number of references: 35

Number of Supplemental Tables: 5

Number of Supplemental Figures: 6

Number of references in Supplemental Materials: 3

Number of words in the Abstract: 235/250

Number of words in the Introduction: 610/750

Number of words in the Discussion: 1,478/1,500

Abbreviations

AUC, area under the curve; DDI, drug–drug interaction; dKO, double knockout; ENT, equilibrative nucleoside transporter; GC-MS, gas chromatography-mass spectrometry; GFR, glomerular filtration rate; HEK293, human embryonic kidney cells 293; LC-MS/MS, liquid

DMD Fast Forward. Published on September 11, 2019 as DOI: 10.1124/dmd.119.087262
This article has not been copyedited and formatted. The final version may differ from this version.

chromatography-tandem mass spectrometry; m^1A, N^1-methyladenosine; MATE, multidrug and toxin exclusion protein; MPP^+, 1-methyl-4-phenylpyridinium; NMN, N^1-methylnicotinamide; OAT, organic anion transporter; OCT, organic cation transporter; PYR, pyrimethamine; SD, standard deviation; SE, standard error of the mean; SNP, single nucleotide polymorphism; TEA, tetraethylammonium; TMAO, trimethylamine-*N*-oxide; WT, wild type

DMD Fast Forward. Published on September 11, 2019 as DOI: 10.1124/dmd.119.087262
This article has not been copyedited and formatted. The final version may differ from this version.

Abstract

Endogenous substrates are emerging biomarkers for drug transporters, which serve as surrogate probes in drug–drug interaction (DDI) studies. In this study, the results of metabolome analysis using wild-type and Oct1/2 double knockout mice suggested that N^1-methyladenosine (m^1A) was a novel OCT2 substrate. An *in vitro* transport study revealed that m^1A is a substrate of mouse Oct1, Oct2, Mate1, human OCT1, OCT2 and MATE2-K, but not human MATE1. Urinary excretion accounted for 77% of the systemic elimination of m^1A in mice. The renal clearance (46.9 ± 4.9 mL/min/kg) of exogenously given m^1A was decreased to near the glomerular filtration rates by Oct1/2 double knockout or Mate1 inhibition by pyrimethamine (16.6 ± 2.6 and 24.3 ± 0.6 mL/min/kg, respectively), accompanied by significantly higher plasma concentrations. *In vivo* inhibition of OCT2/MATE2-K by a single dose of DX-619 in cynomolgus monkeys resulted in the elevation of the area under the curve of m^1A (1.72-fold) as well as metformin (2.18-fold). The plasma m^1A concentration profile showed low diurnal and interindividual variation in healthy volunteers. The renal clearance of m^1A in young (21–45 years old) and older (65–79 years old) volunteers (244 ± 58 and 169 ± 22 mL/min/kg, respectively) was about 2-fold higher than creatinine clearance. The renal clearance of m^1A and creatinine was 31% and 17% smaller in older than young volunteers. Thus, m^1A could be a surrogate probe for the evaluation of DDIs involving OCT2/MATE2-K.

DMD Fast Forward. Published on September 11, 2019 as DOI: 10.1124/dmd.119.087262
This article has not been copyedited and formatted. The final version may differ from this version.

Significance Statement

Endogenous substrates can serve as surrogate probes for clinical drug-drug interaction studies involving drug transporters or enzymes. In this study, N^1-methyladenosine (m^1A) was found as the novel substrate of renal cationic drug transporters, OCT2 and MATE2-K. m^1A was revealed to have some advantages compared to other OCT2/MATEs substrate, creatinine and N^1-methylnicotinamide. The genetic or chemical impairment of OCT2 or MATE2-K caused significant increase of plasma m^1A concentration in mice and cynomolgus monkeys due to the high contribution of tubular secretion to the net elimination of m^1A. Plasma m^1A concentration profile showed low diurnal and interindividual variation in healthy volunteers. Thus, m^1A could be a better biomarker of the variation of OCT2/MATE2-K activity caused by the inhibitory drugs.

Introduction

Drug transporters are one of the key determinants governing drug pharmacokinetics; thus, they provide sites for drug–drug interactions (DDIs) with concomitantly administered drugs. Inhibition of transporters, which facilitate the drug clearance from the systemic circulation, causes an increase in the systemic exposure of substrate drugs and thus could elevate the risk of adverse reactions. To avoid the risk, the regulatory authorities in the United States, the European Union, and Japan have strongly recommended conducting separate clinical studies for investigational inhibitors using probe drugs to firmly evaluate the DDI risks in humans according to their guidelines. Recently, some endogenous substrates have emerged to serve as surrogate probes for clinical DDI studies. Using these endogenous substrates does not require exogenous administration of probe drugs, which enables the early assessment of DDI risks and contributes to overcome the *in vitro–in vivo* gap in the DDI predictions (Mariappan *et al.*, 2017; Chu *et al.*, 2018; Rodrigues *et al.*, 2018).

Organic cation transporter (OCT) 2 is predominantly expressed on the basolateral side of human renal proximal tubular epithelial cells and responsible for the renal influx of water-soluble cationic compounds, such as metformin, tetraethylammonium (TEA), and cisplatin (Morrissey *et al.*, 2013). In turn, the efflux of those drugs into urine is mediated by multidrug and toxin extrusion proteins (MATEs) expressed on the apical side of the proximal tubules (Otsuka *et al.*, 2005; Masuda *et al.*, 2006). Human MATEs have two isoforms, MATE1 and MATE2-K, and they play a key role in the tubular secretion of cationic drugs in cooperation with OCT2. To date, dolutegravir, crizotinib, and vandetanib can inhibit OCT2 at the clinical dose to increase the systemic exposure of metformin (Reese *et al.*, 2013; Johansson *et al.*, 2014; Arakawa *et al.*, 2017). Whereas MATE inhibitors, such as pyrimethamine (PYR), cimetidine, and trimethoprim also reduce renal clearance of metformin (Elsby *et al.*, 2017), and can exacerbate the intracellular accumulation and nephrotoxicity of cisplatin.

We have reported serum creatinine levels and renal clearances of creatinine and N^1-methylnicotinamide (NMN) to reflect the transport activity of OCT2/MATEs using DX-619 and PYR as inhibitors (Imamura *et al.*, 2011; Ito *et al.*, 2012). Indeed, single or multiple doses of OCT2/MATEs inhibitors were reported to be accompanied with an increased level of serum creatinine or reduction in renal creatinine clearances, although some inhibitors did not achieve significant unbound concentrations to inhibit OCT2 and/or MATEs considering their *in vitro* half-maximal inhibitory concentration. Nevertheless, creatinine and NMN have some disadvantages to be utilized as potential biomarkers. Tubular secretion accounts for at most 20% of the renal creatinine clearance (Breyer and Qi, 2010). The plasma concentration of NMN, a metabolite of niacin (or nicotinamide), exhibited a diurnal change and was almost identical between PYR-treated healthy volunteers and the control group, despite of extensive inhibition of the urinary excretion (Ito *et al.*, 2012). Recently it was also reported that trimethylamine-*N*-oxide (TMAO), a carnitine-derived metabolite, is a substrate of OCT2 (Teft *et al.*, 2017) and MATE1 (Gessner *et al.*, 2018). However, the contribution of tubular secretion to the renal clearance of TMAO was not clearly observed in humans based on its renal clearance and the glomerular filtration rate (GFR). Its plasma concentrations also showed extensive diurnal variation, which was presumably caused by food ingestion (Miyake *et al.*, 2017).

To expand our knowledge on the endogenous probes of OCT2/MATEs, we first investigated the novel endogenous substrate of OCT2 by conducting a metabolome analysis using plasma and urine specimens from wild-type (WT) and Oct1/2 double knockout (dKO) mice. After the validation of OCT2/MATEs-mediated transport of the candidate compound, N^1-methyladenosine (m^1A), its utility as a surrogate probe for clinical DDI studies was evaluated in both animals and humans.

DMD Fast Forward. Published on September 11, 2019 as DOI: 10.1124/dmd.119.087262
This article has not been copyedited and formatted. The final version may differ from this version.

Materials and Methods

Materials and Cell Lines

N[1]-methyladenosine was purchased from Carbosynth (Berkshire, UK). [^{3}H]1-methyl-4-phenylpyridinium (MPP^+) (80 Ci/mmol) was obtained from PerkinElmer (Waltham, MA). DX-619 was synthesized in Daiichi-Sankyo Co., Ltd. (Tokyo, Japan). Metformin hydrochloride was purchased from Wako Pure Chemical Industries, Ltd. (Osaka, Japan). All other chemicals and reagents were commercially available and of analytical grade. Human embryonic kidney 293 (HEK293) cells stably expressing mouse OCT1 (mOct1), mOct2, MATE1 (mMate1) and human OCT1 (hOCT1), hOCT2, hMATE1, and hMATE2-K were established and cultured as described previously (Ito *et al.*, 2010).

Animals

Oct1/2 dKO mice (Jonker *et al.*, 2003) were purchased from Taconic Farms (Germantown, NY). FVB/Njcl mice (CLEA Japan, Tokyo, Japan) were employed as Oct1 and Oct2 gene–WT controls. The mice were maintained in an air-conditioned room with lighting at 12 hours intervals, fed a standard animal diet, and received water ad libitum. The mice employed in the current study were from 8 to 12 weeks old. The studies using mice were conducted in accordance with the guidelines provided by the Institutional Animal Care Committee (Graduate School of Pharmaceutical Sciences, The University of Tokyo, Tokyo, Japan).

Three male cynomolgus monkeys at 3 to 4 years old were supplied by Shin Nippon Biomedical Laboratories, Ltd. (Tokyo, Japan). They were housed in a temperature- and humidity-controlled room set to a 12 hours light/dark cycle and given access ad libitum to water and a standard laboratory diet. The study using monkeys was carried out in accordance with the guidelines of the Animal Care and Use Committee of Daiichi-Sankyo Co., Ltd.

Metabolome Analysis

DMD Fast Forward. Published on September 11, 2019 as DOI: 10.1124/dmd.119.087262
This article has not been copyedited and formatted. The final version may differ from this version.

The serum and urine samples from WT and Oct1/2 dKO mice were measured with the Metabolon analytical system (Metabolon Inc., Durham, NC). To identify structurally named and unknown molecules, Metabolon applied a non-targeted semi-quantitative liquid chromatography-tandem mass spectrometry (LC-MS/MS) and gas chromatography-mass spectrometry (GC-MS) platform. Identification codes which start with "X-" were imparted to unnamed metabolites.

In Vitro Transport Study Using cDNA Transfected Cells

Cells were washed and preincubated with Krebs-Henseleit buffer (118 mM NaCl, 23.8 mM $NaHCO_3$, 4.8 mM KCl, 1.0 mM KH_2PO_4, 1.2 mM $MgSO_4$, 12.5 mM HEPES, 5 mM glucose, and 1.5 mM $CaCl_2$) at 37°C for 15 minutes. Then, substrates were added into the wells to initiate the uptake. The pH of the buffer solution was adjusted to 7.4 for OCTs-expressing cells and 8.0 for MATEs-expressing cells. Incubation buffer was removed and ice-cold Krebs-Henseleit buffer was added to halt the uptake at the designated times. For the quantification of m^1A, cells were recovered in 2 mM ammonium acetate (pH 5.0) using a cell scraper and disrupted with a Biorupter (UCD-250HSA; Cosmo Bio, Tokyo, Japan). The specimens were then mixed with a 3-fold volume of methanol for deproteinization and centrifuged for 5 minutes at 20,000 *g*. The supernatant was diluted with a 4-fold volume of 2 mM ammonium acetate (pH 5.0) and subjected to LC-MS/MS analysis. For the quantification of metformin, cells were recovered in 0.1% formic acid and disrupted as well. A 3-fold volume of acetonitrile was added and after centrifugation, the supernatant was subjected to LC-MS/MS analysis. A Pierce BCA Protein Assay Kit (Thermo Fisher Scientific, Waltham, MA) was employed to determine the protein concentration with bovine serum albumin as the protein standard.

Kinetic Analysis of *In Vitro* Data

The data gathered from the saturation study was fitted to the equation below assuming the Michaelis–Menten equation as follows:

DMD Fast Forward. Published on September 11, 2019 as DOI: 10.1124/dmd.119.087262
This article has not been copyedited and formatted. The final version may differ from this version.

$$CL_{uptake} = \frac{V_{max}}{K_m + S}$$

where CL_{uptake} was calculated by subtracting the uptake clearance in the empty vector–overexpressing cells from that in the transporter-expressing ones. V_{max}, S, and K_m represent the maximum transport velocity at saturating substrate concentration, substrate concentrations and the Michaelis constant, respectively.

The inhibition constants of various inhibitors for OCT2 and MATE2-K were calculated using following equation:

$$CL_{uptake(+inhibitor)} = \frac{CL_{uptake(control)}}{1 + I/K_i}$$

where $CL_{uptake\ (+inhibitor)}$ and $CL_{uptake\ (control)}$ indicate the uptake with or without inhibitors, respectively, and I and K_i mean the inhibitor concentration and inhibition constant.

The nonlinear least-squares fitting to calculate kinetic parameters was performed using a MULTI program (Yamaoka *et al.*, 1981) with the damped Gauss–Newton method algorithm.

Transport Study Using Kidney Slices

Slices (300 μm in thickness) of whole kidneys were prepared from WT and Oct1/2 dKO mice, and incubated at 37°C for 5 minutes on a 12-well plate with 1 mL of oxygenated buffer for preincubation. To initiate the uptake, the slices were incubated at 37°C with 1 mL of oxygenated buffer containing 100 μM m^1A for 10 minutes. Then, the slices were rapidly removed from the incubation buffer, washed twice with ice-cold buffer to halt the uptake, blotted on filter paper, and weighed. The specimens were homogenized and deproteinized, followed by the determination of m^1A concentration by LC-MS/MS. The uptake activity of Oct1 and Oct2 in the mouse kidney slices was checked with [^{3}H]MPP^+ as the positive control. To quantify the radiolabeled compound, slices were dissolved in 1 mL of Soluene-350 (Packard Instruments, Meriden, CT) overnight at 55°C. The specimens were mixed with a scintillation cocktail (Hionic Fluor; Packard Instruments)

DMD Fast Forward. Published on September 11, 2019 as DOI: 10.1124/dmd.119.087262
This article has not been copyedited and formatted. The final version may differ from this version.

and the radioactivity in the specimens was determined with a liquid scintillation counter (LS6000SE; Beckman Coulter, Brea, CA).

In vivo Study of m^1A in WT and Oct1/2 dKO Mice

Under anesthesia with isoflurane, m^1A (100 nmol/min/kg) was infused through the jugular vein. Blood samples were obtained through the jugular vein at the indicated times after the initiation of infusion and immediately centrifuged at 12,000 g for 5 minutes to collect plasma fraction. The urethral meatus was fixed with adhesive reagent (Aron Alpha A "Sankyo"; Daiichi-Sankyo Co., Ltd.) to avoid missing urine during the administration period. In the PYR-treatment study, a bolus dose of PYR (20 μmol/kg in saline/ethanol/tween 80 mixture [90/5/5]) was administered via the jugular vein 30 minutes before the initiation of infusion, and rhodamine 123 (1 nmol/min/kg), a typical substrate of mMate1, was infused together with m^1A as the positive control of mMate1 inhibition. At the end of the experiment, urine sample was obtained via urinary bladder and the kidneys were removed. All samples were kept at −20°C until the measurement of m^1A concentration by LC–MS/MS analysis.

Pharmacokinetic Analysis in the Steady-State Infusion Study

The total body clearance ($CL_{tot,\ p}$) and the renal clearance with respect to the plasma concentration ($CL_{r,\ p}$) were obtained as follows:

$$CL_{tot,p} = \frac{Dose}{AUC_p} \quad (1)$$

$$CL_{r,p} = \frac{X_{urine}}{AUC_p} \quad (2)$$

where Dose and X_{urine} indicate the amount of compounds administered in 2 hours and excreted into urine, respectively. AUC_p indicates the area under the time-plasma concentration curve for compounds from 0 to 120 minutes and determined with the trapezoidal rule. The apparent tissue-to-plasma concentration ratio ($K_{p,\ tissue}$) was determined as follows:

DMD Fast Forward. Published on September 11, 2019 as DOI: 10.1124/dmd.119.087262
This article has not been copyedited and formatted. The final version may differ from this version.

$$K_{p,tissue} = \frac{C_{tissue}}{C_p} \quad (3)$$

where C_{tissue} and C_p indicate tissue and plasma concentrations of compounds at 120 minutes after administration, respectively.

In Vivo Inhibition Study of OCT2 and MATEs using DX-619

A crossover study design, where the same three monkeys were employed over a couple of studies, was used with 2 weeks washout period between each study. Monkeys were under overnight fasting condition and then provided food after blood sampling at 6 hours and they were received water ad libitum during the periods. DX-619 (30 mg/kg) in a 0.5% (w/v) methylcellulose (in water) suspension was administered through oral gavage at a dose volume of 5 mL/kg. Adequately 2 hours after the DX-619 administration, metformin was administrated orally at 5 mg/kg (dosing volume: 5 mL/kg) in a 0.5% (w/v) methylcellulose. Blood samples were obtained through the femoral vein collected into tubes coated with heparin at −2 (before metformin dosing), 0.25, 0.5, 1, 2, 4, 6 and 24 hours after metformin dosing. The specimens were kept on ice before being centrifuged to obtain plasma specimens (15,000 rpm, 2 minutes at 4°C). The AUC of test compounds was determined with the trapezoidal rule.

Clinical Samples

The study protocol was approved by the Ethics Review Boards of The University of Tokyo, Kyushu University, and Sugioka Memorial Hospital. Written informed consent was confirmed from all participants prior to their inclusion in this study. The plasma and urine samples were those from our previously performed clinical DDI study (Miyake *et al.*, 2017). Briefly, the study was a single-arm, nonrandomized study where eight young and seven older male subjects were enrolled. All participants were in healthy condition and not on any medication. They received the following drugs in a cassette after overnight fasting for the investigation of the effect of aging to drug transporter activities and cytochrome pigment enzymes, which is the primary objective of

DMD Fast Forward. Published on September 11, 2019 as DOI: 10.1124/dmd.119.087262
This article has not been copyedited and formatted. The final version may differ from this version.

the clinical study: alprazolam 0.2 mg, atorvastatin 3 mg, chlorzoxazone 10 mg, pitavastatin 0.4 mg, telmisartan 5 mg, and valsartan 10 mg. Aliquots of plasma specimens were filtered using Centrifree Ultrafiltration device (Merck Millipore, Burlington, MA) to evaluate the plasma protein binding of m^1A. The participants' information is summarized in **Supplemental Table 1**.

Pharmacokinetic Analysis in the Human Clinical Study

The area under the plasma concentration–time curve from zero to 24 hours ($AUC_{0–24\,h}$) was determined with the trapezoidal rule. The renal clearance with regard to plasma concentration ($CL_{r,\,p}$) of m^1A and creatinine was determined by dividing the amount excreted into the urine from zero to 24 hours ($X_{urine,\,0–24\,h}$) by the $AUC_{0–24\,h}$ value.

$$CL_{r,p} = \frac{X_{urine,0-24\,h}}{AUC_{0-24\,h}} \quad (4)$$

Quantification of Test Compounds in Biological Specimens by LC–MS/MS

The plasma and urine samples were diluted with 10- and 100-fold volume of water, respectively. The kidney specimens were homogenized in a 3-fold volume of saline. For the quantification of m^1A, samples were mixed with a 3-fold volume of methanol and centrifuged at 20,000 *g* for 10 minutes. The supernatants were mixed with a 4-fold volume of 2 mM ammonium acetate (pH 5.0) and subjected to LC–MS/MS analysis. To quantify rhodamine 123 and creatinine, a 3-fold volume of acetonitrile containing 100 nM creatinine-d3 (internal standard) was added followed by the centrifugation and then the supernatant was subjected to LC-MS/MS analysis. Samples were analyzed on QTRAP5500 system (AB SCIEX, Toronto, Canada) equipped with Prominence UFLC (Shimadzu, Kyoto, Japan), operated in electrospray ionization mode. The measurement conditions are summarized in **Supplemental Tables 2 and 3.**

Quantification of Metformin and DX-619 in the Monkey Plasma by LC–MS/MS

DMD Fast Forward. Published on September 11, 2019 as DOI: 10.1124/dmd.119.087262
This article has not been copyedited and formatted. The final version may differ from this version.

Sample analysis was conducted on API 4000 system (AB SCIEX) equipped with ACQUITY UPLC (Waters, Milford, MA), operated in electrospray ionization mode. Each plasma sample was prepared as referred above, followed by mixing with water, acetonitrile, and internal standard solution (niflumic acid 15 ng/mL in acetonitrile / methanol (75:25)). After vortex, the mixtures were filtered employing MultiScreen Solvinert phobic PTFE 0.45 μm (Merck Millipore, Burlington, MA) and transferred to 96-well plates for LC-MS/MS analysis. The measurement conditions are summarized in **Supplemental Table 3.**

Statistical Analysis

Data are presented as the mean ± standard error of the mean (SE) for in vitro and in vivo experiments, and the mean ± standard deviation (SD) for the clinical study. The statistical analysis was performed with Student's t-test and Dunnett's post hoc test to detect significant differences between two groups where appropriate (*$P < 0.05$, **$P < 0.01$, ***$P < 0.001$).

DMD Fast Forward. Published on September 11, 2019 as DOI: 10.1124/dmd.119.087262
This article has not been copyedited and formatted. The final version may differ from this version.

Results

Investigation of Candidate Compounds by Metabolomics Analysis of WT and Oct1/2 dKO Mice

Of 819 compounds surveyed, the compounds which showed higher plasma concentrations or lower urine concentrations in the knockout mice were summarized in **Table 1**. Among them, m^1A was selected for further analysis because its major elimination pathway in rats was urinary excretion (Dutta and Chheda, 1987) and its serum level was significantly associated with OCT2 single nucleotide polymorphisms (SNPs) (Shin *et al.*, 2014).

Uptake of m^1A by Organic Cation Transporters

To verify the m^1A transport by OCT2 and other renal cation transporters, *in vitro* transport study was performed using transporter-overexpressing HEK293 cells. In the m^1A transport studies, 10 μM dipyridamole (an inhibitor of equilibrative nucleoside transporters [ENTs]) was added to the incubation buffer to inhibit ENTs-mediated m^1A uptake in HEK293 cells **(Supplemental Fig. 1A)**. Using [^{3}H]MPP^+ and metformin, it was confirmed that dipyridamole had no effect on OCTs- and MATEs-mediated uptake (**Supplemental Fig. 1B**).

The result is summarized in **Fig. 1**. The m^1A uptake in HEK293 cells individually expressing mOct1, mOct2, and mMate1 was significantly higher than that in empty-vector transfected cells. Among the human transporters, hOCT1, hOCT2, and hMATE2-K were responsible for the uptake of m^1A, but hMATE1 was not. The hOCT2-mediated m^1A transport was not affected by G808T mutation, a well-known SNP of the transporter (Zolk, 2012; Yoon *et al.*, 2013) **(Supplemental Fig. 2)**. The m^1A uptake was not saturated at the concentration of 1 mM for all renal cation transporters other than mMate1, for which K_m and V_{max} values of m^1A were 246 ± 14 μM and 76.7 ± 3.0 pmol/min/mg protein (**Supplemental Fig. 3A and 3B**). Similarly, 1 mM m^1A did not inhibit the metformin uptake by mOct1, mOct2, hOCT2, or

DMD Fast Forward. Published on September 11, 2019 as DOI: 10.1124/dmd.119.087262
This article has not been copyedited and formatted. The final version may differ from this version.

hMATE2-K, although m^1A concentration-dependent inhibition of metformin uptake by mMate1 was observed with the K_i value of 89.5 ± 15.1 μM **(Supplemental Fig. 3C)**.

The K_i values of trimethoprim, PYR, and cimetidine for hOCT2 and hMATE2-K-mediated m^1A uptake were determined **(Fig. 2)**. Concerning substrate dependency, K_i values of these drugs for m^1A uptake were compared with those for creatinine and metformin uptake (Mathialagan *et al.*, 2017) (**Table 2**). Compared to metformin, the K_i value of cimetidine for hOCT2 was 33-times smaller and that of trimethoprim for hMATE2-K was 2.7-fold greater when m^1A was used as the test probe.

m^1A Uptake by Mouse Kidney Slices

Renal cortical slices of WT and Oct1/2 dKO mice were utilized to elucidate the contribution of OCTs to m^1A into the kidney. The effects of Oct1/2 dKO and TEA are shown in **Fig. 3**. The uptake of m^1A into mouse kidney slices was depleted by Oct1/2 dKO or 5 mM TEA, in the same way as [^{3}H]MPP^+ (positive control of the transport activity of OCT). In contrast, it was not affected by 250 μM probenecid, a typical organic anion transporters (OATs) inhibitor.

The Contribution of Oct1/2 to the Kinetics of m^1A in Mice

Plasma concentration of endogenous m^1A was measured using LC-MS/MS in WT and Oct1/2 dKO mice, which were 69.0 ± 6.2 nM and 173 ± 8 nM, respectively (mean ± SE, n = 3, $P < 0.001$). To confirm the key role of Oct1/2 in the clearance and tissue distribution of m^1A *in vivo*, an infusion study was carried out with WT and Oct1/2 dKO mice. The dose of m^1A (100 nmol/min/mg) was selected to achieve concentrations higher than the endogenous level, but below its K_m for mMate1. The kinetic data are shown in **Fig. 4** and **Table 3**. The systemic clearance ($CL_{tot,p}$) was mainly explained by the renal clearance ($CL_{r,p}$) and decreased significantly by Oct1/2 depletion, causing about 2-fold increase of m^1A concentration in the plasma. The $CL_{r,p}$ in Oct1/2 dKO mice was comparable with GFR (Jonker *et al.*, 2003). Regarding the tissue

DMD Fast Forward. Published on September 11, 2019 as DOI: 10.1124/dmd.119.087262
This article has not been copyedited and formatted. The final version may differ from this version.

distribution of m^1A, the kidney to plasma ratio ($K_{p,\ kidney}$) in Oct1/2 dKO mice exhibited a decreasing tendency compared to that in WT mice. On the other hand, the liver to plasma ratio ($K_{p,\ liver}$) was almost equal between these mice.

The Contribution of Mate1 to the Kinetics of m^1A in Mice

We also performed PYR treatment study using WT mice to check the contribution of Mate1 to the renal secretion of m^1A. PYR was administered to mice by a bolus injection 30 minutes prior to the initiation of the m^1A infusion, considering the long half-life of PYR in the systemic circulation (Ito *et al.*, 2010). The dosage amount of PYR (20 μmol/kg) was chosen to inhibit mMate1 strongly as reported previously (Kito *et al.*, 2018). A reference Mate1 substrate, rhodamine 123 was simultaneously given to mice with m^1A. The kinetic change of m^1A by PYR treatment is summarized in **Fig. 5** and **Table 4**. The $CL_{r,\ p}$ of m^1A was significantly lower in the PYR-treated group, which caused the decrease of $CL_{tot,\ p}$. PYR treatment also caused the elevation of the $K_{p,\ kidney}$ of m^1A, as well as that of rhodamine 123. The plasma concentration of m^1A was about 1.5-fold higher in the PYR-treated group, while PYR did not affect that of rhodamine 123.

Effect on DX-619 on the Kinetics of m^1A and Metformin in Monkeys

To elucidate the significance of OCT2 and MATE2-K on the m^1A kinetics in primates, a single-dose study was carried out with male cynomolgus monkeys administered metformin with or without DX-619, which inhibits those transporters at its therapeutic dose. Prior to this study, m^1A transport by cynomolgus monkey OCT2 was confirmed using cDNA transfected HEK293 cells (**Supplemental Fig. 4**).

Plasma-concentration profiles of m^1A, metformin, creatinine and DX-619 after oral administration of metformin (5 mg/kg) with and without DX-619 pretreatment (30 mg/kg) are summarized in **Fig. 6**. DX-619 dose (30 mg/kg, p.o.) was designed to achieve sufficient plasma concentrations exceeding by far the reported K_i value (0.94 μM) for hOCT2-mediated creatinine

DMD Fast Forward. Published on September 11, 2019 as DOI: 10.1124/dmd.119.087262
This article has not been copyedited and formatted. The final version may differ from this version.

uptake (Imamura *et al.*, 2011). The administration of DX-619 resulted in an increase in the AUC_p of m^1A and metformin (**Table 5**), though not statistically significant ($p = 0.06$ and 0.07, respectively). The plasma concentration of creatinine exhibited an increasing tendency in the DX-619-treated period.

Determination of the Renal Clearance of m^1A and Creatinine in Young and Older Volunteers

To obtain insight into the dispersion of m^1A in human, m^1A and creatinine concentrations in the plasma and urine samples from young and older healthy volunteers were determined with LC-MS/MS. Binding of m^1A to the plasma protein was not detected. As is the case with creatinine, the plasma concentration profile of m^1A showed low diurnal and interindividual variation, and no significant difference between the young and older subjects. The amount of m^1A excreted into urine was significantly lower in older subjects **(Fig. 7A)**, leading to the reduction in renal clearance **(Table 6)**. The AUC of plasma m^1A concentration and creatinine clearance were in the moderate negative correlation **(Fig. 7B, left panel)**. The renal clearance of m^1A was about 2-fold higher than creatinine clearance **(Table 6)** and they also showed a moderate correlation **(Fig. 7B, right panel)**.

DMD Fast Forward. Published on September 11, 2019 as DOI: 10.1124/dmd.119.087262
This article has not been copyedited and formatted. The final version may differ from this version.

Discussion

Endogenous substrates were recently regarded as surrogate probes for the clinical assessment of DDI risk in drug development. OCT2 and MATEs are the major drug transporters involved in the proximal tubular secretion of organic cations, although sensitive and convenient biomarkers for them have not been found yet. Therefore, the goal of this study was to identify the novel endogenous metabolites in the plasma that could be utilized in DDI studies for renal OCT2/MATEs in healthy subjects.

We employed Oct1/2 dKO mice for the metabolomic analysis to search the candidate metabolites because OCT1 is also expressed in the basolateral membrane of proximal tubular epithelial cells along with OCT2 in mice. m^1A was suggested to be the potential probe and subjected to the further analysis. It should be noted that N^6-methyladenosine (m^6A) has the same *m/z* transition as m^1A in LC-MS/MS analysis. For that reason, we optimized the analytical condition in which analyte peaks of m^1A and m^6A are detected separately (**Supplemental Table 1**) and could reproduce the significant alteration of plasma m^1A concentration in Oct1/2 dKO mice. m^6A concentration was under the lower limit of quantification (3 nM) in any specimen. Plasma concentrations of various kinds of fatty acids were also higher in Oct1/2 dKO mice. However, it was assumed to be the effect of Oct1 knockout, which causes hepatic thiamine deficiency and thereby enhances fatty acid oxidation to compensate the reduced glycolysis (Chen *et al.*, 2014).

m^1A is the modified nucleoside that originally presents at the position 58 in transfer RNA (tRNA). For the stabilization of tRNA tertiary structure, the N^1 position of adenine 58 is methylated to introduce the positive charge into TψC loop of tRNA. Under cell stress conditions, tRNA is damaged to get unfolded and then enzymatically cleaved into tRNA-derived stress-induced RNA (tiRNA), followed by the degradation to mononucleosides including m^1A (Mishima *et al.*, 2014). We considered another possibility for the synthesis of m^1A, such as direct methylation of adenosine by gut flora, which motivated us to compare the endogenous level of

m^1A in plasma and various tissues between germ-free mice and specific-pathogen-free mice (**Supplemental Fig. 5**). The result showed no significant difference in the plasma, liver, and kidney concentrations, whereas significant difference in the intestine and decreasing tendency in the brain were observed. On the other hand, the abundance of TMAO, whose precursor trimethylamine is produced by gut flora-mediated metabolism, was diminished in germ-free mice, indicating that the contribution of gut flora to the m^1A disposition is negligible. In addition, in all tissues tested, endogenous m^1A was detected at about 10-fold higher concentration than in plasma.

In vitro transport study revealed that m^1A is a substrate of not only mOct2 and hOCT2, but also mOct1, mMate1, hOCT1 and hMATE2-K (**Fig. 1**). Except for mMate1 with K_m value of 246 ± 14 μM, renal cation transporter-mediated m^1A uptake was not saturated even at the concentration of 1 mM (**Supplemental Fig. 3**), indicating the low-affinity and high-capacity nature of m^1A transport by those transporters. Considering the substrate dependency of K_i values (Hacker *et al.*, 2015; Lechner *et al.*, 2016; Mathialagan *et al.*, 2017), we compared the K_i values of the three inhibitors for m^1A uptake with those for other typical substrates. Trimethoprim and PYR exhibited almost identical inhibition constants for all substrates, whereas the K_i value of cimetidine varied according to each substrate. Further studies are necessary whether this finding is *in vivo* relevant in future clinical studies.

Next, we investigated the physiological significance of OCTs in m^1A transport with Oct1/2 dKO mice. We have clarified that TEA-sensitive uptake of m^1A was completely abolished in the kidney slices from Oct1/2 dKO mice (**Fig. 3**). The results of the infusion study show that the systemic clearance of m^1A was dominated mostly by the urinary excretion. Approximately 80% of intravenously given m^1A was recovered unchanged in the urine in WT mice. The renal clearance of m^1A was decreased to the value comparable with the GFR in Oct1/2 dKO mice (**Table 3**), causing its accumulation in the plasma (**Fig. 4**). A decreasing tendency of the $K_{p,kidney}$ of m^1A was observed in Oct1/2 dKO mice, but there was a too large variation in this parameter in WT mice to obtain statistical significance by unknown reason. In contrast, the $K_{p,liver}$ was much

lower than $K_{p,kidney}$ and almost identical between WT and Oct1/2 dKO mice, indicating little contribution of mOct1 to the hepatic uptake of m^1A. Importance of mMate1 in the urinary excretion of m^1A was suggested by *in vivo* study using a MATE1 inhibitor PYR. PYR significantly decreased renal clearance of m^1A, accompanied by the increased kidney-to-plasma ratio and plasma concentration of m^1A (**Fig. 5**), attributable to a significant reduction in the luminal efflux. On the other hand, the kinetics of exogenously given m^1A was almost identical between WT and Mdr1a/1b/Abcg2 triple knockout mice (**Supplemental Fig. 6 and Supplemental Table 4**), confirming the predominant role of mMate1 in the efflux of m^1A across the brush border membrane in mice.

Recently, cynomolgus monkeys are utilized as a surrogate model to evaluate pharmacokinetic changes by the inhibition of renal drug transporters (Tahara *et al.*, 2006; Shen *et al.*, 2016). Monkey cation transporters exhibit the high similarity to their human counterparts represented by amino acid sequence, transport properties such as substrate selectivity and pH dependency, and inhibition constants of various inhibitors (Shen *et al.*, 2016). In accordance, intravenous infusion of PYR caused the reduction of metformin renal clearance in cynomolgus monkeys (Shen *et al.*, 2016) as is the case for oral PYR pretreatment in humans (Kusuhara *et al.*, 2011). In our study, administration of DX-619, a potent OCT2 and MATE1/2-K inhibitor, resulted in the increase of AUC_p of both m^1A and metformin (**Fig. 6**), indicating the potency of plasma m^1A concentration as a biomarker for the evaluation of OCT2/MATE2-K mediated DDIs. This is the salient feature not found in other endogenous substrates of OCT2/MATEs such as N^1-methylnicotinamide and creatinine. Plasma concentration is practically the better biomarker than renal clearance or urinary recovery, considering the simplicity of sample collection. The plasma creatinine concentration also exhibited an increasing tendency in the DX-619-treated period. Although metformin was eliminated from the systemic circulation at 24 hours after DX-619 administration, the plasma creatinine concentration remained high. Considering that the serum elimination half-life of creatinine (3.85 hours; Chiou and Hsu, 1975) is shorter than metformin

(4.0–8.7 hours (Dunn and Peters, 1995)) in humans—of course, further studies in cynomolgus monkeys are needed—there might be other mechanisms to alter the kinetics of creatinine.

Finally, we investigated the time profiles of plasma concentration and urinary excretion of m^1A and creatinine in healthy young and older volunteers (**Fig. 7** and **Table 6**). Like creatinine, the plasma concentrations of m^1A showed minimal diurnal variation for 24 hours. The renal clearance of m^1A was revealed to be approximately 2-fold higher than that of creatinine, indicating greater contribution of the tubular secretion to the net urinary excretion of m^1A. Correlation analysis suggested that m^1A AUC and renal clearance reflected renal function including OCT2/MATE2-K activity. The renal clearance of m^1A and creatinine was 31% and 17% lower in older volunteers than in young volunteers, respectively. Probably that is why the plasma m^1A concentrations were slightly higher in older volunteers, although it was not the case with creatinine.

The major challenge remaining is to examine the effect of OCT2/MATE2-K inhibitors or genetic variants on m^1A kinetics in humans. It was previously reported that the serum m^1A level was significantly associated only with genetic variants of OCT2 in the metabolomic and genome-wide association study (Shin *et al.*, 2014), whereas nonsynonymous SNP in the coding region was not included in those variants (**Supplemental Table 5**). In accordance with genome-wide association study, no effect of G808T mutation on hOCT2-mediated m^1A uptake was observed *in vitro* (**Supplemental Fig. 2**). To conclude the performance of m^1A as surrogate probe of OCT2 and MATE2-K needs further clinical studies using inhibitors of them.

In addition, the contribution of other transporters to the disposition of m^1A remains to be revealed. In our experiment, ENTs-mediated m^1A uptake was observed in HEK293 parental cells (**Supplemental Fig. 1A**). Although ENTs did not appear to have major roles in the renal secretion of m^1A in mice, the effect of ENTs inhibition on the systemic exposure of m^1A needs further investigation, considering the ubiquitous expression of ENTs (Young *et al.*, 2013). The m^1A transport by OATs expressing in basolateral membrane of proximal tubular cells must also be

DMD Fast Forward. Published on September 11, 2019 as DOI: 10.1124/dmd.119.087262
This article has not been copyedited and formatted. The final version may differ from this version.

checked, which we could not precisely evaluate using transporter-overexpressing HEK293 cells because of the inhibition of OATs by dipyridamole (data not shown).

In conclusion, we found m^1A was a novel endogenous substrate of OCT2 and MATE2-K. m^1A is a renal excretion type compound that undergoes tubular secretion via those transporters in animals and humans. This study has provided the potency of m^1A as a biomarker for OCT2/MATE2-K in future clinical DDI studies.

Authorship Contributions

Participated in research design: Miyake, Mizuno, Ieiri, Maeda, Kusuhara.

Conducted experiments: Miyake, Takehara, Mochizuki, Kimura, Matsuki, Irie, Watanabe, Ando.

Contributed analytic tools or new reagents: Kato.

Performed data analysis: Miyake, Takehara, Watanabe, Ando, Kusuhara.

Contributed to or wrote the writing of the manuscript: Miyake, Mizuno, Takehara, Ando, Kusuhara.

References

Arakawa H, Omote S, and Tamai I (2017) Inhibitory Effect of Crizotinib on Creatinine Uptake by Renal Secretory Transporter OCT2. *J Pharm Sci* **106**:2899–2903.

Breyer MD, and Qi Z (2010) Better nephrology for mice—and man. *Kidney Int* **77**:487–489.

Chen L, Shu Y, Liang X, Chen EC, Yee SW, Zur AA, Li S, Xu L, Keshari KR, Lin MJ, Chien H-C, Zhang Y, Morrissey KM, Liu J, Ostrem J, Younger NS, Kurhanewicz J, Shokat KM, Ashrafi K, and Giacomini KM (2014) OCT1 is a high-capacity thiamine transporter that regulates hepatic steatosis and is a target of metformin. *Proc Natl Acad Sci U S A* **111**:9983–8.

Chiou WL and Hsu FH (1975) Pharmacokinetics of Creatinine in Man and Its Implications in the Monitoring of Renal Function and in Dosage Regimen Modifications in Patients with Renal Insufficiency. *J Clin Pharmacol* **15**:427–434.

Chu X, Liao M, Shen H, Yoshida K, Zur AA, Arya V, Galetin A, Giacomini KM, Hanna I, Kusuhara H, Lai Y, Rodrigues D, Sugiyama Y, Zamek-Gliszczynski MJ, and Zhang L (2018) Clinical Probes and Endogenous Biomarkers as Substrates for Transporter Drug-Drug Interaction Evaluation: Perspectives From the International Transporter Consortium. *Clin Pharmacol Ther* **104**:836–864.

Dunn CJ and Peters DH (1995) Metformin. A review of its pharmacological properties and therapeutic use in non-insulin-dependent diabetes mellitus. *Drugs* **49**:721–749.

Dutta SP and Chheda GB (1987) Metabolism of 1-methyladenosine. *Biochem Med Metab Biol* **38**:69–73.

Elsby R, Chidlaw S, Outteridge S, Pickering S, Radcliffe A, Sullivan R, Jones H, and Butler P (2017) Mechanistic in vitro studies confirm that inhibition of the renal apical efflux transporter multidrug and toxin extrusion (MATE) 1, and not altered absorption, underlies the increased metformin exposure observed in clinical interactions with cimetidine, trimethoprim or pyrimethamine. *Pharmacol Res Perspect* **5**:e00357.

Gessner A, König J, and Fromm MF (2018) Contribution of multidrug and toxin extrusion protein 1 (MATE1) to renal secretion of trimethylamine-N-oxide (TMAO). *Sci Rep* **8**:6659.

Hacker K, Maas R, Kornhuber J, Fromm MF, and Zolk O (2015) Substrate-Dependent Inhibition of the Human Organic Cation Transporter OCT2: A Comparison of Metformin with Experimental Substrates. *PLoS One* **10**:e0136451.

Imamura Y, Murayama N, Okudaira N, Kurihara A, Okazaki O, Izumi T, Inoue K, Yuasa H, Kusuhara H, and Sugiyama Y (2011) Prediction of Fluoroquinolone-Induced Elevation in Serum Creatinine Levels: A Case of Drug–Endogenous Substance Interaction Involving the Inhibition of Renal Secretion. *Clin Pharmacol Ther* **89**:81–88.

Ito S, Kusuhara H, Kumagai Y, Moriyama Y, Inoue K, Kondo T, Nakayama H, Horita S, Tanabe K, Yuasa H, and Sugiyama Y (2012) N-Methylnicotinamide Is an Endogenous Probe for Evaluation of Drug–Drug Interactions Involving Multidrug and Toxin Extrusions (MATE1 and MATE2-K). *Clin Pharmacol Ther* **92**:635–641.

Ito S, Kusuhara H, Kuroiwa Y, Wu C, Moriyama Y, Inoue K, Kondo T, Yuasa H, Nakayama H, Horita S, and Sugiyama Y (2010) Potent and Specific Inhibition of mMate1-Mediated Efflux of Type I Organic Cations in the Liver and Kidney by Pyrimethamine. *J Pharmacol Exp Ther* **333**:341-50.

Johansson S, Read J, Oliver S, Steinberg M, Li Y, Lisbon E, Mathews D, Leese PT, and Martin P (2014) Pharmacokinetic Evaluations of the Co-Administrations of Vandetanib and Metformin, Digoxin, Midazolam, Omeprazole or Ranitidine. *Clin Pharmacokinet* **53**:837–847.

Jonker JW, Wagenaar E, Van Eijl S, and Schinkel AH (2003) Deficiency in the Organic Cation Transporters 1 and 2 (Oct1/Oct2 [Slc22a1/Slc22a2]) in Mice Abolishes Renal Secretion of Organic Cations. *Mol Cell Biol* **23**:7902–7908.

Kito T, Ito S, Mizuno T, Maeda K, and Kusuhara H (2018) Investigation of non-linear Mate1-mediated efflux of trimethoprim in the mouse kidney as the mechanism underlying drug-drug interactions between trimethoprim and organic cations in the kidney. *Drug Metab Pharmacokinet*, doi: 10.1016/J.DMPK.2018.08.005.

Kusuhara H, Ito S, Kumagai Y, Jiang M, Shiroshita T, Moriyama Y, Inoue K, Yuasa H, and Sugiyama Y (2011) Effects of a MATE Protein Inhibitor, Pyrimethamine, on the Renal Elimination of Metformin at Oral Microdose and at Therapeutic Dose in Healthy Subjects. *Clin Pharmacol Ther* **89**:837–844.

Lechner C, Ishiguro N, Fukuhara A, Shimizu H, Ohtsu N, Takatani M, Nishiyama K, Washio I, Yamamura N, and Kusuhara H (2016) Impact of Experimental Conditions on the Evaluation of Interactions between Multidrug and Toxin Extrusion Proteins and Candidate Drugs. *Drug Metab Dispos* **44**:1381–9.

Mariappan TT, Shen H, and Marathe P (2017) Endogenous Biomarkers to Assess Drug-Drug Interactions by Drug Transporters and Enzymes. *Curr Drug Metab* **18**:757-768.

Masuda S, Terada T, Yonezawa A, Tanihara Y, Kishimoto K, Katsura T, Ogawa O, and Inui K (2006) Identification and functional characterization of a new human kidney-specific H+/organic cation antiporter, kidney-specific multidrug and toxin extrusion 2. *J Am Soc Nephrol* **17**:2127–35.

Mathialagan S, Rodrigues AD, and Feng B (2017) Evaluation of Renal Transporter Inhibition Using Creatinine as a Substrate In Vitro to Assess the Clinical Risk of Elevated Serum Creatinine. *J Pharm Sci* **106**:2535–2541.

Mishima E, Inoue C, Saigusa D, Inoue R, Ito K, Suzuki Y, Jinno D, Tsukui Y, Akamatsu Y, Araki M, Araki K, Shimizu R, Shinke H, Suzuki T, Takeuchi Y, Shima H, Akiyama Y, Toyohara T, Suzuki C, Saiki Y, Tominaga T, Miyagi S, Kawagisihi N, Soga T, Ohkubo T, Yamamura K, Imai Y, Masuda S, Sabbisetti V, Ichimura T, Mount DB, Bonventre J V, Ito

S, Tomioka Y, Itoh K, and Abe T (2014) Conformational change in transfer RNA is an early indicator of acute cellular damage. *J Am Soc Nephrol* **25**:2316–26.

Miyake T, Mizuno T, Mochizuki T, Kimura M, Matsuki S, Irie S, Ieiri I, Maeda K, and Kusuhara H (2017) Involvement of Organic Cation Transporters in the Kinetics of Trimethylamine N-oxide. *J Pharm Sci* **106**:2542–2550.

Morrissey KM, Stocker SL, Wittwer MB, Xu L, and Giacomini KM (2013) Renal Transporters in Drug Development. *Annu Rev Pharmacol Toxicol* **53**:503–529.

Otsuka M, Matsumoto T, Morimoto R, Arioka S, Omote H, and Moriyama Y (2005) A human transporter protein that mediates the final excretion step for toxic organic cations. *Proc Natl Acad Sci* **102**:17923–17928.

Reese MJ, Savina PM, Generaux GT, Tracey H, Humphreys JE, Kanaoka E, Webster LO, Harmon KA, Clarke JD, and Polli JW (2013) In vitro investigations into the roles of drug transporters and metabolizing enzymes in the disposition and drug interactions of dolutegravir, a HIV integrase inhibitor. *Drug Metab Dispos* **41**:353–61.

Rodrigues A, Taskar K, Kusuhara H, and Sugiyama Y (2018) Endogenous Probes for Drug Transporters: Balancing Vision With Reality. *Clin Pharmacol Ther* **103**:434–448.

Shen H, Liu T, Jiang H, Titsch C, Taylor K, Kandoussi H, Qiu X, Chen C, Sukrutharaj S, Kuit K, Mintier G, Krishnamurthy P, Fancher RM, Zeng J, Rodrigues AD, Marathe P, and Lai Y (2016) Cynomolgus Monkey as a Clinically Relevant Model to Study Transport Involving Renal Organic Cation Transporters: In Vitro and In Vivo Evaluation. *Drug Metab Dispos* **44**:238–49.

Shin S-Y, Fauman EB, Petersen A-K, Krumsiek J, Santos R, Huang J, Arnold M, Erte I, Forgetta V, Yang T-P, Walter K, Menni C, Chen L, Vasquez L, Valdes AM, Hyde CL, Wang V, Ziemek D, Roberts P, Xi L, Grundberg E, Waldenberger M, Richards JB, Mohney RP, Milburn M V, John SL, Trimmer J, Theis FJ, Overington JP, Suhre K,

Brosnan MJ, Gieger C, Kastenmüller G, Spector TD, Soranzo N, and Soranzo N (2014) An atlas of genetic influences on human blood metabolites. *Nat Genet* **46**:543–550.

Tahara H, Kusuhara H, Chida M, Fuse E, and Sugiyama Y (2006) Is the monkey an appropriate animal model to examine drug-drug interactions involving renal clearance? Effect of probenecid on the renal elimination of H2 receptor antagonists. *J Pharmacol Exp Ther* **316**:1187–94.

Teft WA, Morse BL, Leake BF, Wilson A, Mansell SE, Hegele RA, Ho RH, and Kim RB (2017) Identification and Characterization of Trimethylamine-N-oxide Uptake and Efflux Transporters. *Mol Pharm* **14**:310–318.

Yamaoka K, Tanigawara Y, Nakagawa T, and Uno T (1981) A pharmacokinetic analysis program (multi) for microcomputer. *J Pharmacobiodyn* **4**:879–85.

Yoon H, Cho H-Y, Yoo H-D, Kim S-M, and Lee Y-B (2013) Influences of Organic Cation Transporter Polymorphisms on the Population Pharmacokinetics of Metformin in Healthy Subjects. *AAPS J* **15**:571–580.

Young JD, Yao SYM, Baldwin JM, Cass CE, and Baldwin SA (2013) The human concentrative and equilibrative nucleoside transporter families, SLC28 and SLC29. *Mol Aspects Med* **34**:529–547.

Zolk O (2012) Disposition of metformin: Variability due to polymorphisms of organic cation transporters. *Ann Med* **44**:119–129.

Footnotes

This study was supported partly by Grants-in-Aid for Scientific Research foundation B from Japan Society for the Promotion of Science [17H04100], a grant of Long-range Research Initiative (LRI) by Japan Chemical Industry Association (JCIA) [grant no. 13_PT03-01-3], and by Grants-in-Aid for Clinical Pharmacology Research Foundation Award from the Japanese Society of Clinical Pharmacology and Therapeutics.

DMD Fast Forward. Published on September 11, 2019 as DOI: 10.1124/dmd.119.087262
This article has not been copyedited and formatted. The final version may differ from this version.

Figure Legends

Figure 1. In vitro transport study of m^1A.

The uptake of m^1A (100 μM) by organic cation transporters was determined in the absence (solid line) or presence (dotted line) of inhibitor (5 mM tetraethylammonium (TEA)). The incubation buffer also contained 10 μM dipyridamole to inhibit the ENTs-mediated m^1A uptake. Each symbol and bar represent the mean ± SE (n = 3). *$P < 0.05$, **$P < 0.01$, ***$P < 0.001$, the absence vs. presence of 5 mM TEA in transporter-overexpressing cells, Student's two-tailed unpaired t-test.

Figure 2. Effect of various inhibitors on hOCT2- and hMATE2-K-mediated m^1A uptake.

The uptake of m^1A (100 μM) for 60 minutes in HEK293 cells stably expressing hOCT2 or hMATE2-K was determined in the absence and presence of inhibitors (trimethoprim, pyrimethamine, cimetidine) at the designated concentrations. The transporter-specific uptake of m^1A was calculated by subtracting the uptake by empty vector–transfected cells from that by transporter-expressing cells and shown as a proportion to the uptake value in the absence of inhibitors. The solid line represents the fitted line obtained by nonlinear regression analysis as described in the ***Materials and Methods***. Each symbol and bar represent the mean ± SE (n = 3).

Figure 3. m^1A uptake by renal cortical slices of WT and Oct1/2 dKO mouse

The uptake of m^1A (100 μM) for 10 min in renal cortical slices of wild-type (WT) mice and Oct1/2 double knockout (dKO) mice was determined in the absence or presence of 250 μM probenecid or 5 mM TEA. Each bar represents the mean ± SE (n = 3). **$P < 0.01$, Dunnett's post hoc test.

Figure 4. m^1A infusion assay using WT and Oct1/2 dKO mice.

Effect of Oct1/2 dKO on the plasma and concentrations and urinary excretion of exogenously given m^1A (100 nmol/min/kg) in mice. The kinetic parameters were calculated as described in

DMD Fast Forward. Published on September 11, 2019 as DOI: 10.1124/dmd.119.087262
This article has not been copyedited and formatted. The final version may differ from this version.

Materials and Methods. Each symbol and bar represent the mean and SE (n = 3). **P* < 0.05, ***P* < 0.01, Student's two-tailed unpaired t-test.

Figure 5. Effect of PYR on the kinetics of m^1A in mice.

Plasma concentrations and urinary excretion of m^1A were determined in control and PYR-treated mice. PYR (20 μmol/kg) was given to mice by a bolus injection 30 minutes before starting the intravenous infusion of m^1A (100 nmol/min/kg) and rhodamine 123 (1 nmol/min/kg). The kinetic parameters were calculated as described in ***Materials and Methods***. Each symbol and bar represent the mean and SE (n = 4). **P* < 0.05, ***P* < 0.01, ****P* < 0.001, Student's two-tailed unpaired t-test.

Figure 6. In vivo inhibition study of OCT2 and MATEs using DX-619.

Plasma concentration profiles of m^1A, metformin, creatinine and DX-619 after oral administration of metformin (5 mg/kg) with (□) and without (■) DX-619 pretreatment (30 mg/kg) in cynomolgus monkeys were determined. Each symbol and bar represent the mean and SE (n = 3). P-value was calculated by Student's two-tailed paired t-test.

Figure 7. Plasma concentrations and the renal clearance of m^1A in young and older volunteers.

Plasma concentration profiles and the urinary excretion of m^1A and creatinine in young and older volunteers were determined. Each symbol and bar represent the mean ± SD of eight and seven subjects. **P* < 0.05, ***P* < 0.01, ****P* < 0.001, Young vs. Older, Student's two-tailed unpaired t-test.

DMD Fast Forward. Published on September 11, 2019 as DOI: 10.1124/dmd.119.087262
This article has not been copyedited and formatted. The final version may differ from this version.

Tables

Table 1. List of endogenous compounds of interest in the metabolomics analysis performed in wild-type (WT) and Oct1/2 double knockout (dKO) mice

Identity	Platform	Protonated Molecule	Fold Change (Oct1/2 dKO/WT)	
			Plasma	Urine
Pipecolate	LC-MS Pos	130.1	1.43***	1.1
Cadaverine	GC-MS	174	N/A	0.43*
3-methylglutarylcarnitine	LC-MS Pos	290.1	2.65**	1.9
S-methylcysteine	GC-MS	162.1	1.04	0.54*
Putrescine	GC-MS	174	0.93	0.62**
Docosahexaenoate	LC-MS Neg	327.3	1.35**	N/A
Dihomolinolenate	LC-MS Neg	305.4	1.26*	N/A
Arachidonate	LC-MS Neg	303.4	1.28*	N/A
Docosapentaenoate	LC-MS Neg	329.4	2.23**	N/A
Mead acid	LC-MS Neg	305.4	1.51**	N/A
12,13-DiHOME	LC-MS Neg	313.4	1.69**	N/A
Choline	LC-MS Pos	104.2	1.21*	N/A
1-docosahexaenoylglycerophosphocholine	LC-MS Pos	568.4	1.14*	N/A
1-docosahexaenoyl-glycerophosphoethanolamine	LC-MS Neg	524.3	1.31*	N/A
N^1-methyladenosine	LC-MS Pos	282.1	2.78**	0.84
3-ureidopropionate	LC-MS Pos	133.1	0.55*	0.66*
Glycolate (hydroxyacetate)	GC-MS	177	1.23*	1.19
X-11478	LC-MS Neg	165.2	2***	N/A
X-11909	LC-MS Neg	297.3	1.86**	N/A
X-12257	LC-MS Neg	269.1	3.13*	0.77

DMD Fast Forward. Published on September 11, 2019 as DOI: 10.1124/dmd.119.087262
This article has not been copyedited and formatted. The final version may differ from this version.

X-16570	LC-MS Neg	198.2	2.95*	1.29
X-16575	LC-MS Neg	293.1	2.04***	N/A
X-16581	LC-MS Pos	304.1	2.36***	2.77**
X-17307	LC-MS Pos	162.1	N/A	0.48**
X-18628	LC-MS Pos	931.4	2.16*	N/A
X-20568	LC-MS Pos	188.1	N/A	0.56*

Table 2. Comparison of in vitro inhibition constant of various drugs for OCT2- and MATE2-K- mediated uptake

Each value was determined from the data shown in **Fig. 2**. The equations for calculation are described in ***Materials and Methods*.** Each value represents the mean ± computer-calculated SD.

Inhibitors	hOCT2 (μM)			hMATE2-K (μM)		
	m^1A 100 μM	Creatinine 100 μM	Metformin 10 μM	m^1A 100 μM	Creatinine 100 μM	Metformin 10 μM
Trimethoprim	20 ± 5	26 ± 2	20 ± 2	2.4 ± 0.4	0.58 ± 0.11	0.92 ± 0.04
Pyrimethamine	0.64 ± 0.18	0.93 ± 0.04	0.61 ± 0.04	0.22 ± 0.06	0.35 ± 0.05	0.22 ± 0.02
Cimetidine	1.8 ± 0.4	36 ± 3	59 ± 1.4	5.3 ± 1.6	24 ± 5	5.2 ± 0.8

DMD Fast Forward. Published on September 11, 2019 as DOI: 10.1124/dmd.119.087262
This article has not been copyedited and formatted. The final version may differ from this version.

Table 3. Pharmacokinetic parameters of m^1A in WT and Oct1/2 dKO mice

The equations to calculate the kinetic parameters are described in ***Materials and Methods*.** Each value represents the mean ± SE (n = 3). **P* < 0.05, ***P* < 0.01, ****P* < 0.001, Student's two-tailed unpaired t-test; value in Oct1/2 dKO mice vs. WT mice.

	[unit]	Wild type	Oct1/2 dKO	
$C_{p,\ 120\ min}$	[μM]	1.63 ± 0.23	2.45 ± 0.11	*
$AUC_{p,\ 0–120\ min}$	[μmol*min/L]	138 ± 15	203 ± 9	*
X_{urine}	[nmol]	220 ± 27	103 ± 13	*
C_{liver}	[μM]	3.31 ± 0.49	5.63 ± 0.28	*
$K_{p,\ liver}$	[mL/g liver]	2.08 ± 0.36	2.30 ± 0.09	
C_{kidney}	[μM]	15.6 ± 6.7	9.27 ± 0.91	
$K_{p,\ kidney}$	[mL/g kidney]	8.81 ± 2.70	3.76 ± 0.23	
$CL_{tot,\ p}$	[mL/min]	2.10 ± 0.13	1.11 ± 0.04	**
	[mL/min/kg]	61.1 ± 2.7	36.4 ± 1.3	**
$CL_{r,\ p}$	[mL/min]	1.61 ± 0.16	0.511 ± 0.077	**
	[mL/min/kg]	46.9 ± 4.9	16.6 ± 2.6	**
GFR (Jonker *et al.*, 2003)	[mL/min]	0.462 ± 0.045	0.462 ± 0.065	

Table 4. Pharmacokinetic parameters of m^1A and rhodamine 123 in control and PYR-treated mice

The equations to calculate the kinetic parameters are described in ***Materials and Methods*.** Each value represents the mean ± SE (n = 4). **P* < 0.05, ***P* < 0.01, ****P* < 0.001, Student's two-tailed unpaired t-test; value in control mice vs. PYR-treated mice.

	m^1A			Rhodamine 123		
	Control	PYR	[unit]	Control	PYR	[Unit]
$C_{p,\ 120\ min}$	1.64 ± 0.10	2.31 ± 0.13**	[μM]	5.61 ± 0.46	5.01 ± 0.39	[nM]
$AUC_{p,\ 0–120\ min}$	140 ± 9	182 ± 11*	[μmol*min/L]	564 ± 27	512 ± 12	[nmol*min/L]
X_{urine}	170 ± 10	126 ± 5**	[nmol]	477 ± 32	21.2 ± 3.4***	[pmol]
C_{kidney}	7.22 ± 1.82	34.0 ± 5.4**	[μM]	0.800 ± 0.074	1.86 ± 0.21	[μM]
$K_{p,\ kidney}$	4.4 ± 1.1	14.7 ± 2.0**	[mL/g kidney]	143 ± 6	381 ± 70	[mL/g kidney]
$CL_{tot,\ p}$	2.32 ± 0.12	1.78 ± 0.13*	[mL/min]	3.93 ± 0.18	4.07 ± 0.05	[mL/min]
	80.4 ± 4.9	61.9 ± 3.6*	[mL/min/kg]	136 ± 8	142 ± 2	[mL/min/kg]
$CL_{r,\ p}$	1.23 ± 0.11	0.698 ± 0.035**	[mL/min]	0.851 ± 0.073	0.0416 ± 0.0073	[mL/min]
	42.6 ± 4.1	24.3 ± 0.6**	[mL/min/kg]	29.6 ± 3.1	1.44 ± 0.21	[mL/min/kg]
GFR (Jonker *et al.*, 2003)	0.462 ± 0.045	0.462 ± 0.065	[mL/min]			

Table 5. The AUC of metformin and m^1A in control and DX-619-treated monkeys

		1	2	3	Mean ± SE	Unit
m^1A	Control	364	216	219	266 ± 49	nM*h
	+DX-619	468	361	464	431 ± 35	
	Fold change	1.29	1.67	2.12	1.72±0.24	
Metformin	Control	43.5	11.1	38.3	31.0 ± 10.0	μM*h
	+DX-619	91.9	26.5	77.6	65.3 ± 19.9	
	Fold change	2.11	2.39	2.03	2.18±0.11	

Table 6. Pharmacokinetic parameters of m^1A in young and older Japanese volunteers

Each value was determined from the data shown in **Fig. 7**. The equations to calculate the kinetic parameters are described in ***Materials and Methods***. Each value represents the mean ± SD of eight and seven subjects. $^{**}P < 0.01$, $^{***}P < 0.001$, Student's two-tailed unpaired t-test; Young vs. Older. Subject information is shown in **Supplemental Table 4**.

	m^1A			Creatinine		
	Young	Older	[Unit]	Young	Older	[Unit]
$AUC_{0–24\ h}$	1.22 ± 0.22	1.29 ± 0.14	[μmol*h/L]	1.05 ± 0.12	1.04 ± 0.16	[mmol*h/L]
$X_{urine,\ 0\text{-}24\ h}$	17.2 ± 1.4	13.0 ± 0.9***	[μmol]	8.06 ± 0.79	6.61 ± 1.17	[mmol]
$CL_{r,p}$	244 ± 58	169 ± 22**	[mL/min]	129 ± 18	108 ± 21	[mL/min]

DMD Fast Forward. Published on September 11, 2019 as DOI: 10.1124/dmd.119.087262
This article has not been copyedited and formatted. The final version may differ from this version.

Figures

Figure 1

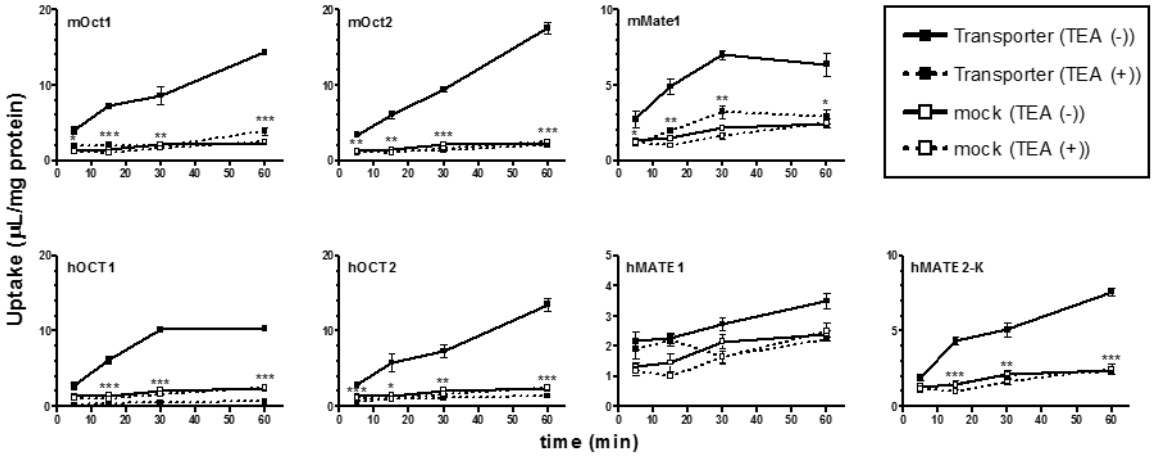

Figure 2

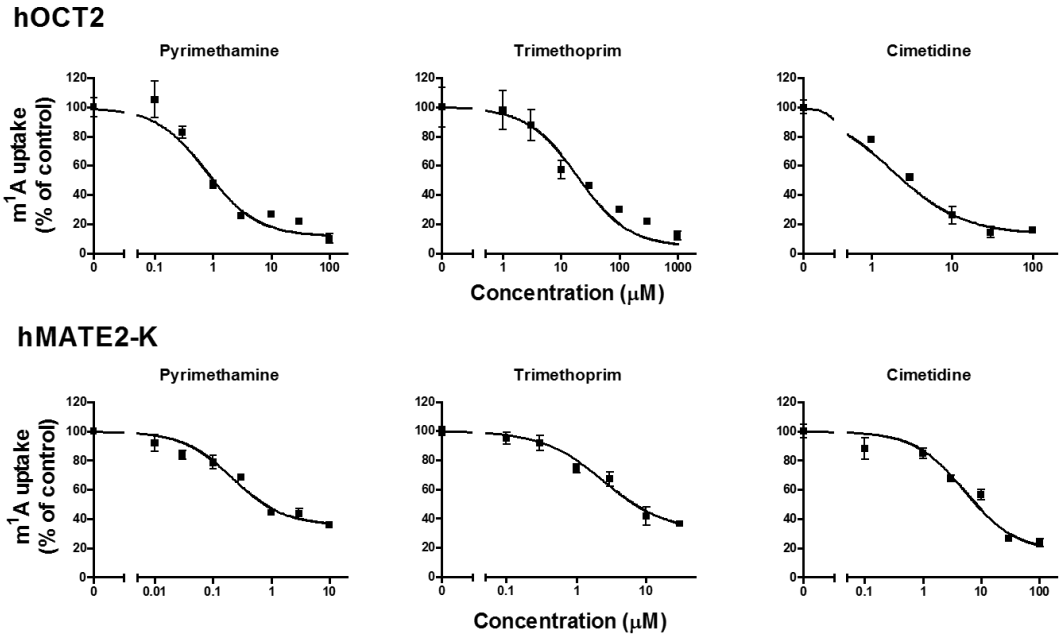

DMD Fast Forward. Published on September 11, 2019 as DOI: 10.1124/dmd.119.087262
This article has not been copyedited and formatted. The final version may differ from this version.

Figure 3

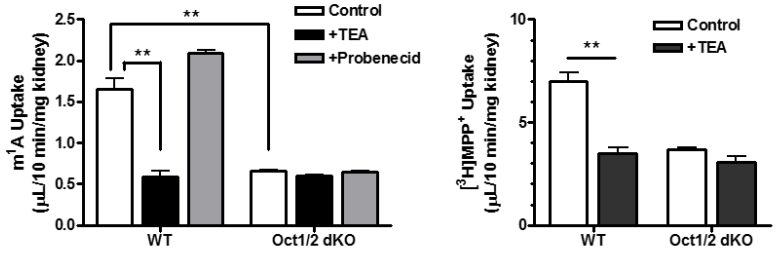

Figure 4

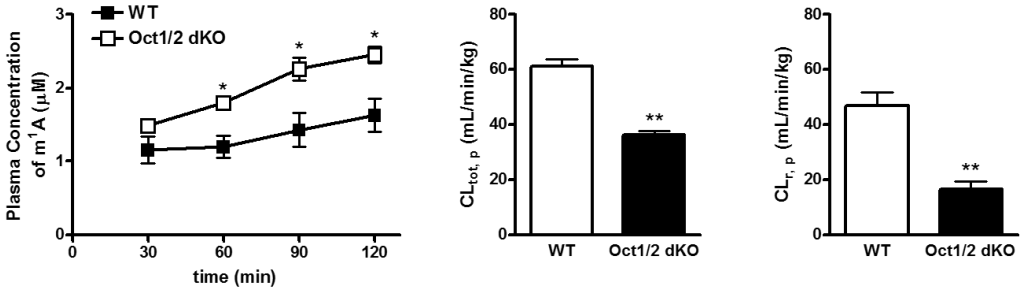

Figure 5

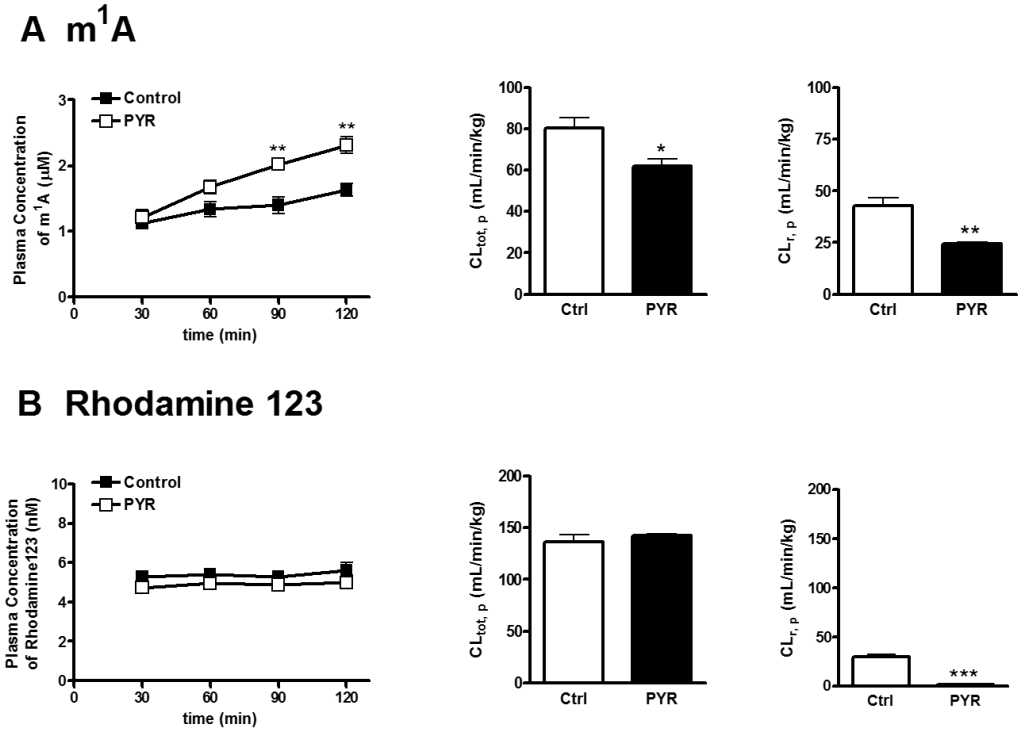

Figure 6

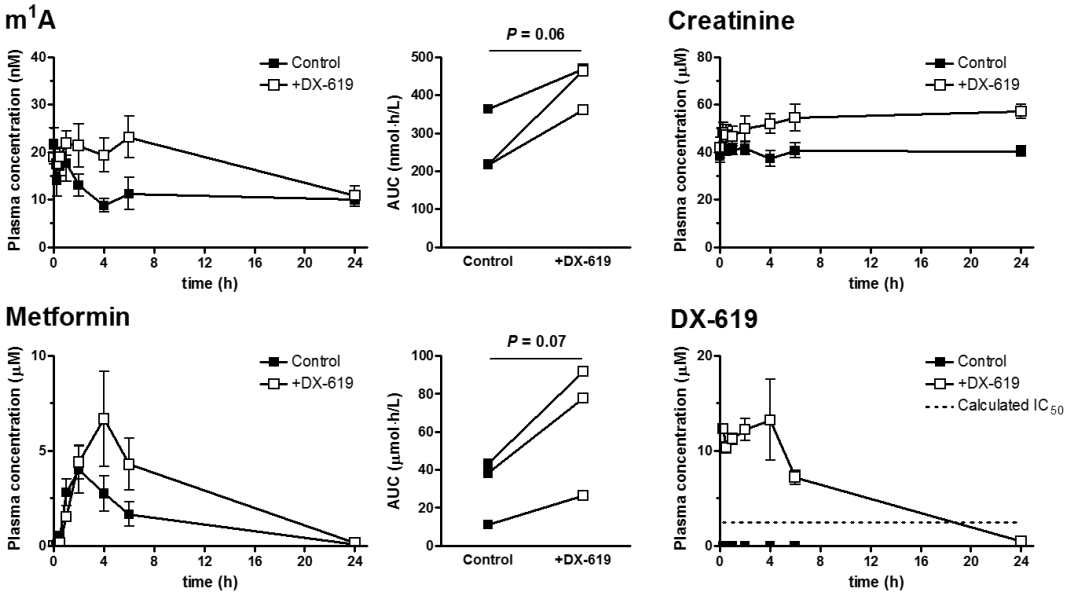

DMD Fast Forward. Published on September 11, 2019 as DOI: 10.1124/dmd.119.087262
This article has not been copyedited and formatted. The final version may differ from this version.

Figure 7